# Supplemental Materials for

## Non-linear chiral rheology of a phospholipid monolayer

*KyuHan Kim, Siyoung Q. Choi, Joseph A. Zasadzinski, and Todd M. Squires*

### Pre-shear

The nonlinear elastic response is complicated by an initial slip between domains along grain boundaries (Fig. S1 1-5). To eliminate these effects, we begin each measurement by applying a pre-torque that causes domains to initially slip, then deform elastically. When the external torque is removed, the elastically-deformed domains relax, but do not return completely to their original configuration, leaving some residual strain behind (Fig. S1 1-3). Subsequent torques, applied in the same direction, deform the domains without this initial slip, so that complete strain recovery is observed, and repeatable elastic modulus measurements can be

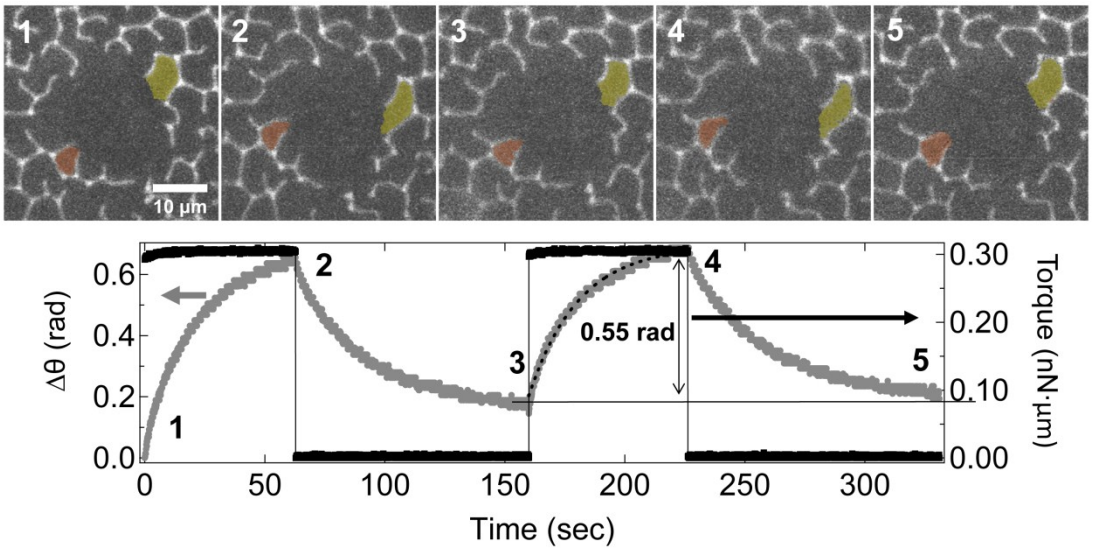


**Fig. S1** Procedure for pre-shearing and annealing the monolayer so that subsequent strains are fully recovered after removing the external torque.

made (Fig. S1 3-5). Relatively low torque (~ 0.3 nN·μm) is applied to LC domains (1) to deform the domains in a clockwise direction, as indicated by the deformed green and brown domains. When the external force is balanced by a restoring force due to the strain on the domains (2), the external force is removed, and the system relaxes. Due to the dissipation between sliding domains (brown domain), however, the micro-button initially does not return entirely to its original position (3). In order to obtain fully recovered strain, subsequent external torque is applied in the clockwise direction again until the angular displacement reaches to the plateau (4), and this process is followed by relaxation upon removing the external force (5). Black dots are the fitted result of exponential function to the angular displacement (~ 0.55 rad), which fully recovers the strain in 4-5 subsequent processes.

## Relating the Torque to the Yield Radius

To relate a constant rotation speed, $\Omega$ (radians/sec) to the yield radius, $R_y$, we assume conservation of total torque, $T_0$:

$$2\pi\tau_{r\theta}r^2 = 2\pi\mu_s r^3\frac{\partial}{\partial r}\left(\frac{v_\theta}{r}\right) = -T_0 \qquad \text{(S1)}$$

For a constant surface shear viscosity, $\mu_s$, (at a given surface pressure in a given direction), the velocity field, $v_\theta$ is:

$$v_\theta = Ar + \frac{T_0}{2\pi\mu_s}\frac{1}{2r} \qquad \text{(S2)}$$

At the yield radius, $R_y$, $v_\theta = 0$, which determines $A$:

$$A = -\frac{T_0}{2\pi\mu_s}\frac{1}{2R_y^2} \qquad \text{(S3)}$$

which gives:

$$v_\theta = \frac{-T_0}{4\pi\mu_s}\left(\frac{r}{R_y^2} - \frac{1}{r}\right) \tag{S4}$$

The velocity at the edge of the disc at $r = a$ is $\Omega a$:

$$\Omega a = \frac{-T_0}{4\pi\mu_s}\left(\frac{a}{R_y^2} - \frac{1}{a}\right) \tag{S5}$$

Solving for the total torque, $T_0$:

$$T_0 = 4\pi\mu_s\Omega\left(\frac{a^2R_y^2}{R_y^2 - a^2}\right) \tag{S6}$$

At the yield radius, $R_y$, the torque is defined to be:

$$T_0 = Y_s 2\pi R_y^2 = 4\pi\mu_s\Omega\left(\frac{a^2R_y^2}{R_y^2 - a^2}\right) \tag{S7}$$

in which $Y_s$ is the surface yield stress. Simplifying this expression gives:

$$Y_s = 2\mu_s\Omega\left(\frac{a^2}{R_y^2 - a^2}\right) \tag{S8}$$

which is rearranged to give the expression plotted in Fig. 2d:

$$\frac{R_y^2 - a^2}{a^2} = \frac{2\mu_s}{Y_s}\Omega \tag{S9}$$

The slope of the line plotted in Fig. 2d is $2\mu_s/Y_s$.

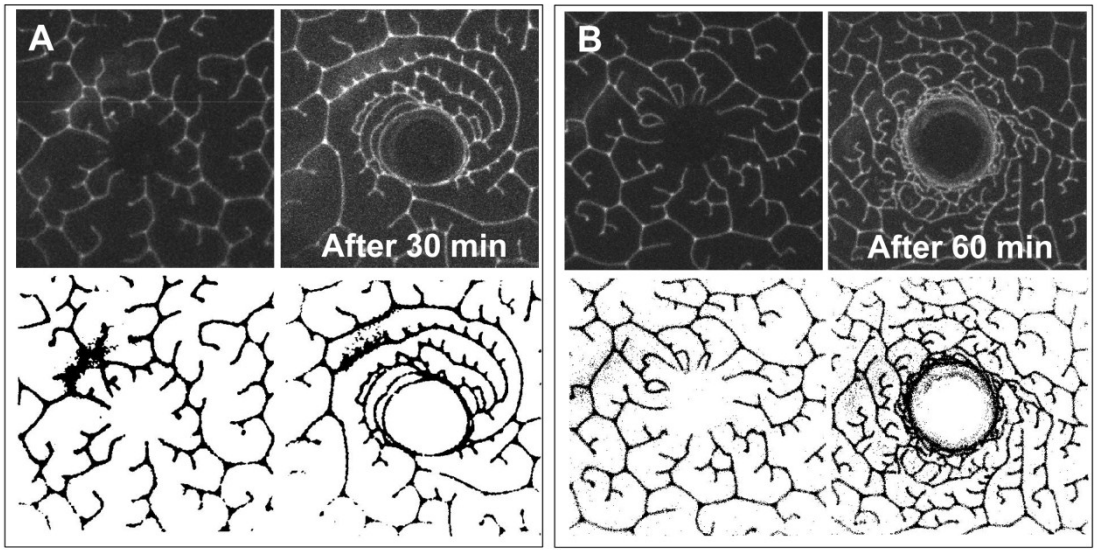


**Fig. S2 (a)** r-DPPC monolayer before and 30 minutes after C-torque cessation (top). Contrast inverted image from top to facilitate measurement of defect line length. By 30 minutes, the total line length in both images is ~ 800 μm**. (b)** r-DPPC monolayer before and 60 minutes after CC-torque cessation. The total line length prior to shear was ~ 1000 μm, but was ~ 1500 μm even after 60 minutes of healing.

## "Healing" the Monolayer

C-torqued monolayers heal over the course of about 30 minutes as indicated by the restoration of the length of bright defect lines. Fig. S2a shows the before torque and after 30 minutes after torque ended for the C-torqued sample. The contrast in the bottom images is reversed (defect lines are black) in a white background to highlight the defect lines and simplify measuring the total length. The total line length ($L_{ToT}$) for the original monolayer (A, left) is ~ *800 μm*. After 30 minutes of healing, $L_{ToT}$ has returned to ~ *800 μm*. In S2B, the original undistorted monolayer has $L_{ToT}$ ~ *1000 μm*, but even after 60 minutes following CC-

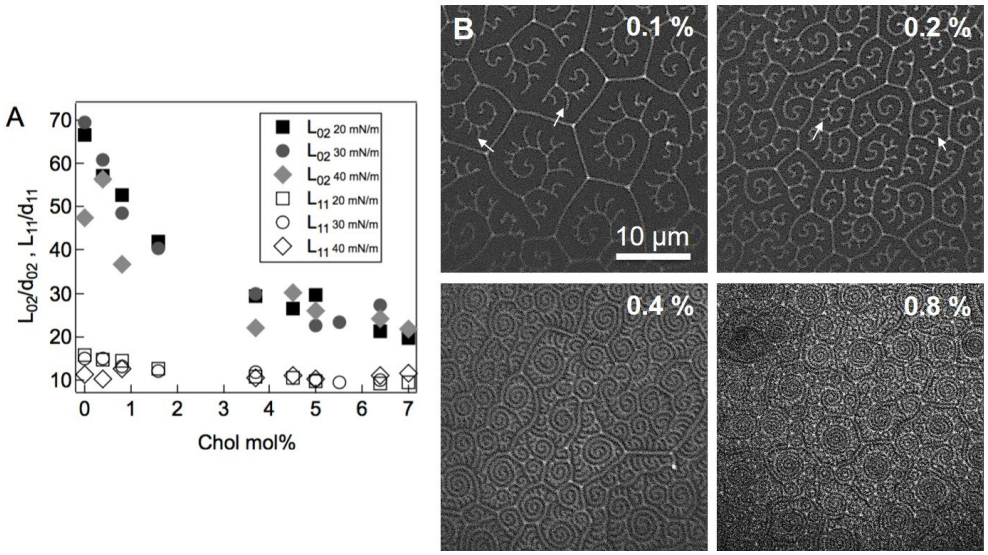


**Fig. S3 (a)** Grazing incidence X-ray diffraction measurement of the correlation length in the $L_{02}$, untilted direction and the $L_{11}$, tilted direction in monolayers of DPPC mixed with cholesterol (Redrawn after Ref. 1[11] in terms of the lattice repeat spacings, $d_{02}$ and $d_{11}$. Adding cholesterol decreases the lattice correlation lengths. **(b)** Fluorescence images of DPPC monolayers in the liquid condensed phase with increasing cholesterol mole fraction. The short bright lines (small arrows) show the segregation of the fluorescent lipid dye to the likely terminations of the tilt gradient lines[3,4], which are only on the convex side of the longer domain boundary lines as in Fig. 5. The spacing of the short bright lines decreases with increasing cholesterol fraction for the 0.1 and 0.2% samples, consistent with a decreased spacing of the tilt gradient lines and increasing domain twist. For higher cholesterol fractions, the tilt gradient lines are not visible, but the rotation of the domains increases. This suggests that as the correlation length decreases, the spacing between tilt gradient lines increases, consistent with the de Gennes analogy to the Landau-Ginzberg parameter in superconductors.

torque, healing is still in progress and $L_{ToT}$~ *1500 μm.* Once the defect lines have formed, it appears to be a very slow process to anneal these lines.

## Correlation Length and Domain Rotation in r-DPPC – Cholesterol Mixtures and the deGennes Analogy

de Gennes showed that chiral twist or bend distortions in layered materials are mathematically analogous to the application of a magnetic field to a superconductor[1]. As in superconductors, there are two characteristic lengths, a coherence or correlation length, $\xi$, which is related to the core radius for dislocations in a lattice, or the length over which lattice correlations decay as in Fig. S3. The second length scale is the chiral penetration depth, $\lambda$. de Gennes describes this length as the depth of the penetration of a weak twist or bend deformation at the free surface into the material. If the ratio, $\kappa = \lambda/\xi$ or "Landau-Ginzburg" parameter is $< 1/\sqrt{2}$, the magnetic field (or twist or bend deformation) is expelled (type-I behavior) from the superconductor or molecular lattice. However, if $> 1/\sqrt{2}$, the magnetic field is incorporated into the Abrikosov flux lattice (type-II behavior) or the twist or bend deformation is incorporated into an array of edge dislocations that form the tilt gradient lines in Fig. S3[1]. The network of edge dislocations in the tilt gradient lines preserves the regular layer or lattice spacing except at the tilt boundaries at which there is a jump in the tilt orientation. Brewster angle[2] and polarized fluorescence microscopy[3–5] confirm the tilt orientation is uniform over the lobes of DPPC domains, with discontinuous jumps across "tilt-gradient" lines. Hatta[6] showed that edge dislocations find it energetically favorable to localize to form these tilt gradient lines. Following plastic deformation of the monolayer, the mobile dislocations re-align over time to restore the tilt gradient lines, as in Fig. 5[6]. We speculate that the spiral rotation imposed by the chiral center of DPPC in Fig.S3 is established by a regular spacing of these dislocation-mediated tilt gradient lines[3,4].

While screw dislocations are not possible in monolayer films, they are involved in a related twist grain boundary phase in smectic A* liquid crystals. In chiral smectic A* phases, a regular array of screw dislocations divides the smectic layers into blocks that are rotated relative to adjoining layer blocks by a discrete amount[7,8]. This rotation results in a macroscopic helical structure in the plane of the layers, with the layering preserved within each smectic block, and the twist is localized to the screw dislocations array that make up the twist grain boundaries. The Twist Grain Boundary (TGB) model of the smectic A* phase also uses a Landau-Ginzberg criteria to set the regular spacing of the twist grain boundaries by defining the twist penetration length relative to the smectic layer correlation length.

Expulsion of chiral twist is also observed in two-dimensional colloidal monolayers composed of rod-shaped, but naturally chiral viruses[9]. The rod-shaped virus align to form monolayers, wherein the rods are oriented normal to the layer everywhere but at free edges, where rods twist to be parallel to the monolayer in relieve the frustrated chirality, over a distance related to the twist penetration length in the de Gennes or TGB theory[1,9,10]. The orientation of the virus at the free edge leads to variations in the line tension, which may be similar to the anisotropic line tension of the chiral domains of r-DPPC[9,10].

We speculate that the regular separation of the bright lines in Fig. 5 and in S3b, which are likely the termination of tilt gradient lines, is sect by the appropriate Landau-Ginzberg parameter. The chiral twist imposed by r-DPPC creates a penetration depth for reorientation of the tilt, which is opposed by the correlation length of the tilted molecular lattice of r-DPPC (Fig. S3a). Fig. S3b shows that the rotation of the domains in r-DPPC monolayers, is increased by adding small amounts (0.1 – 4 mol%) of cholesterol, and the separation between the bright lines, or tilt gradient lines, is decreased. Fig. S3a shows that the added cholesterol decreases the correlation length of the lattice[11] but the twist penetration length likely remains

the same, since the r-DPPC headgroup lattice is unchanged. This suggests that the Landau-Ginzberg parameter, $\kappa = \lambda/\xi$ increases with increasing cholesterol fraction and decreasing $\xi$. This combination would move the transition where $\kappa > 1/\sqrt{2}$ which would decrease the the distance between tilt gradient lines, which in turn would lead to more rotation of the domains, as seen in Fig. S3b.

## References


1 P. G. de Gennes, *Solid State Commun.*, 1972, **10**, 753–756.

2 V. T. Moy, D. J. Keller, H. E. Gaub and H. H. McConnell, *J. Phys. Chem.*, 1986, **90**, 3198–3202.

3 J. Dreier, J. Brewer and A. C. Simonsen, *Soft Matter*, 2012, **8**, 4894.

4 J. Dreier, J. Brewer and A. C. Simonsen, *Langmuir*, 2014, **30**, 10678–10685.

5 U. Bernchou, J. Brewer, H. S. Midtiby, J. H. Ipsen, L. A. Bagatolli and A. C. Simonsen, *J. Am. Chem. Soc.*, 2009, **131**, 14130–1.

6 E. Hatta, *Langmuir*, 2015, **31**, 9597–9601.

7 K. J. Ihn, J. A. N. Zasadzinski, R. Pindak, A. J. Slaney and J. Goodby, *Science (80-. ).*, 1992, **258**, 275–278.

8 J. Fernsler, L. Hough, R.-F. Shao, J. E. Maclennan, L. Navailles, M. Brunet, N. V Madhusudana, O. Mondain-Monval, C. Boyer, J. Zasadzinski, J. A. Rego, D. M. Walba and N. A. Clark, *Proc. Natl. Acad. Sci. U. S. A.*, 2005, **102**, 14191–6.

9 T. Gibaud, E. Barry, M. J. Zakhary, M. Henglin, A. Ward, Y. Yang, C. Berciu, R. Oldenbourg, M. F. Hagan, D. Nicastro, R. B. Meyer and Z. Dogic, *Nature*, 2012, **481**, 348–351.

10 C. N. Kaplan and R. B. Meyer, *Soft Matter*, 2014, **10**, 4700–4710.

11 S. Q. Choi, K. Kim, C. M. Fellows, K. D. Cao, B. Lin, K. Y. C. Lee, T. M. Squires and J. A. Zasadzinski, *Langmuir*, 2014, **30**, 8829–8838.